

# Determination of the absolute stereochemistry and the activation barriers of thermally interconvertible heterocyclic compounds bearing a naphthyl substituent

Öznur Demir-Ordu, Esra Müjde Yılmaz and İlknur Doğan\*

*Boğaziçi University, Chemistry Department, Bebek, 34342 Istanbul, Turkey*

Received 14 September 2005; accepted 28 September 2005

Available online 9 November 2005

**Abstract**—The enantiotopic methyl signals of the compounds studied were resolved in the presence of the optically active chiral auxiliary (*S*)-(+)-2,2,2-trifluoroanthryl ethanol, [(*S*)-TFAE] via complex formation between (*S*)-TFAE and the respective compounds. Two different solvation models were proposed for both **M** and **P** conformations leading to the assignments of the <sup>1</sup>H NMR signals and thus absolute conformations. The solvation models proposed also explained the strong temperature dependence of the <sup>1</sup>H NMR signals upon cooling. The activation barriers for interconversion between the enantiomers of the compounds studied have been determined by either temperature dependent NMR or enantioresolution on a chiral sorbent via HPLC.  
© 2005 Elsevier Ltd. All rights reserved.

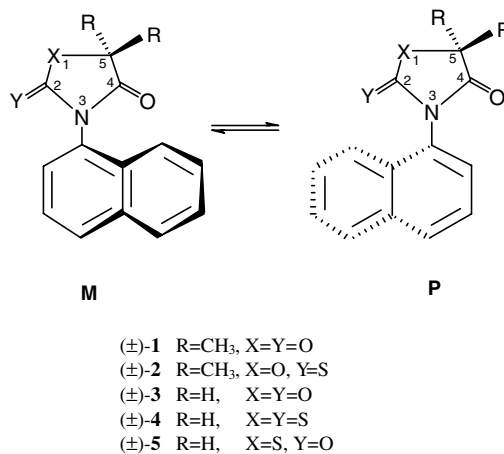
## 1. Introduction

Supramolecular interactions such as hydrogen bonding and  $\pi$  stacking between aromatic rings play an important role in diverse areas such as the stereochemistry of organic reactions,<sup>1</sup> and host–guest chemistry.<sup>2,3</sup> The dependence of spectroscopic properties on these type of interactions has been used for the determination of absolute stereochemistries for many years.<sup>4,5</sup> Diastereometric association complexes formed through these kind of interactions of chiral molecules show non-identical spectral behaviour on the NMR time scale. With knowledge of the structures of the solvates and on the basis of non-equivalence, absolute stereochemistries can be determined.

Recently, we proposed a solvation model for the determination of the absolute conformations of the 5,5-dimethyl-3-(*o*-aryl)-2,4-oxazolidinedione enantiomers.<sup>6</sup> In this model, the solute enantiomers interact with (*S*)-(+)-2,2,2-trifluoroanthryl ethanol, (*S*)-TFAE, in three ways: (1) a two-point interaction complex formed with the lactone part of the ring, (2) an association of the (*S*)-TFAE hydroxyl proton with the amide carbonyl

oxygen present and (3) the existing  $\pi$ – $\pi$  interaction between the aromatic rings.

The importance of a  $\pi$ – $\pi$  interaction between the *o*-substituted phenyl ring of the compounds studied,<sup>6</sup> and the anthryl ring of the chiral auxiliary led us to synthesize a series of axially chiral heterocyclic compounds bearing a naphthyl ring (Scheme 1), which can be involved in enhanced  $\pi$  stacking interactions with the



**Scheme 1.** The compounds synthesized.

\* Corresponding author. Tel.: +90 212 359 6620; fax: +90 212 287 2467; e-mail: dogan@boun.edu.tr

anthryl ring of the (*S*)-TFAE. In these compounds, axial chirality arises from hindered rotation around the C<sub>sp<sup>2</sup></sub>–N<sub>sp<sup>2</sup></sub> single bond and makes the compounds enantiomers.<sup>7</sup>

Herein, we are concerned about the details of interactions between enantiomeric naphthyl substituted compounds (Scheme 1) and (*S*)-TFAE revealed by a strong temperature dependence of the <sup>1</sup>H NMR spectra of the diastereomeric association complexes, which was not observed for the *ortho*-aryl substituted compounds of the same series. This led us to investigate the possibility of determining the absolute conformations of the enantiomers by an NMR method in the presence of an optically active auxiliary. Herein, we also report the activation barriers to the hindered rotation of the compounds studied, determined either by temperature dependent NMR or by thermal racemization on a chiral sorbent via HPLC.

## 2. Results and discussion

### 2.1. <sup>1</sup>H and <sup>13</sup>C NMR

The naphthyl bearing heterocyclic compounds exist as two enantiomeric **M** and **P** atropisomers (Scheme 1), which exhibit identical NMR spectra in an achiral solvent. However, due to hindered rotation around the C<sub>sp<sup>2</sup></sub>–N<sub>sp<sup>2</sup></sub> single bond, the C-5 methyl protons of the compounds 5,5-dimethyl-3-( $\alpha$ -naphthyl)-2,4-oxazolidinedione ( $\pm$ )-**1** and 5,5-dimethyl-3-( $\alpha$ -naphthyl)-2-thioxo-4-oxazolidinone ( $\pm$ )-**2** and the C-5 protons of the compounds 3-( $\alpha$ -naphthyl)-2,4-oxazolidinedione ( $\pm$ )-**3**, 3-( $\alpha$ -naphthyl)-rhodanine ( $\pm$ )-**4**, 3-( $\alpha$ -naphthyl)-2,4-thiazolidinedione ( $\pm$ )-**5** are diastereotopically related and should have unequal chemical shifts if the barrier to rotation is slow on the NMR time scale. Analysis of the <sup>1</sup>H and <sup>13</sup>C NMR spectra of these compounds did show these magnetically non-equivalent protons (Table 1). The two methyl groups on C-5 in compounds ( $\pm$ )-**1** and ( $\pm$ )-**2** gave two separate singlets in toluene-*d*<sub>8</sub> with a chemical shift difference of 0.04 ppm. The protons at C-5 of ( $\pm$ )-**3**, ( $\pm$ )-**4** and ( $\pm$ )-**5** on the other hand, showed AB type splittings, the chemical shift differences being equal to 0.06, 0.07 and 0.06 ppm, respectively. The anisochronous <sup>13</sup>C nuclei of the C-5 methyl groups in

compounds ( $\pm$ )-**1** and ( $\pm$ )-**2** also gave two distinct singlets in toluene-*d*<sub>8</sub>, with same chemical shift difference of 0.6 ppm. These results proved that there was a restricted rotation around the C<sub>sp<sup>2</sup></sub>–N<sub>sp<sup>2</sup></sub> bond making this bond a chiral axis.

### 2.2. <sup>1</sup>H NMR in the presence of a chiral auxiliary

The existence of the two enantiomeric forms for compounds ( $\pm$ )-**1–5** was also proven by <sup>1</sup>H NMR spectroscopy in the presence of 6 equiv of (*S*)-(+)-2,2,2-trifluoroanthryl ethanol, (*S*)-TFAE. Enantiomeric groups become diastereotopic by non-equivalent interactions with (*S*)-TFAE as proposed previously,<sup>6</sup> and thus displayed unequal <sup>1</sup>H NMR chemical shifts.

In the <sup>1</sup>H NMR spectra of ( $\pm$ )-**1** the expected four singlets of the C-5 methyl groups were observed in the presence of (*S*)-TFAE with a chemical shift difference of 0.01 ppm for the upfield and 0.02 ppm for the downfield pair of the signals in toluene-*d*<sub>8</sub> (Fig. 1). For compound ( $\pm$ )-**2** however, only one enantiomeric pair for the C-5 methyl groups was distinguished under the same conditions. The two separated singlets appeared downfield with a chemical shift difference of 0.01 ppm in toluene-*d*<sub>8</sub> (Fig. 1).

In the presence of (*S*)-TFAE, the two expected AB splittings were differentiated on the NMR time scale for the C-5 methylene protons of compounds ( $\pm$ )-**3** and ( $\pm$ )-**5**, with the chemical shift difference being equal to 0.02 ppm for the downfield and 0.01 ppm for upfield pair of the signals (Fig. 1). The two AB splittings for the C-5 methylene protons of compound ( $\pm$ )-**4** were also observed with a chemical shift difference of 0.02 ppm for the downfield signals; however the upfield part of the spectrum could not be resolved (Fig. 1D).

With these results in hand, it was concluded that the existence of the –C=S group on C-2 [compounds ( $\pm$ )-**2** and ( $\pm$ )-**4**] decreases the resolution of the enantiomeric pairs of these compounds compared to the –C=O analogues. The observed decrease in the resolution for the enantiomeric upfield signals may arise from a structural change in the solvation model that will be discussed later.

**Table 1.** <sup>1</sup>H and <sup>13</sup>C NMR spectroscopic data for the synthesized compounds in the presence and absence of the optically active auxiliary, (*S*)-TFAE at 30 °C

Compound no.	Medium	<sup>1</sup> H NMR, ppm, C-5 methyl	<sup>1</sup> H NMR, ppm, C-5 protons	<sup>13</sup> C NMR, ppm, C-5 methyl
( $\pm$ )- <b>1</b>	Toluene- <i>d</i> <sub>8</sub>	1.28 and 1.24	—	28.9 and 28.3
	Toluene- <i>d</i> <sub>8</sub> +( <i>S</i> )-TFAE <sup>a</sup>	1.35, 1.33, 1.30, 1.29	—	—
( $\pm$ )- <b>2</b>	Toluene- <i>d</i> <sub>8</sub>	1.27 and 1.23	—	28.6 and 28.0
	Toluene- <i>d</i> <sub>8</sub> +( <i>S</i> )-TFAE <sup>a</sup>	1.37, 1.36 and 1.31	—	—
( $\pm$ )- <b>3</b>	Toluene- <i>d</i> <sub>8</sub>	—	3.07 and 3.01	—
	Toluene- <i>d</i> <sub>8</sub> +( <i>S</i> )-TFAE <sup>a</sup>	—	3.06, 3.04, 2.98, 2.97	—
( $\pm$ )- <b>4</b>	Toluene- <i>d</i> <sub>8</sub>	—	3.04 and 2.97	—
	Toluene- <i>d</i> <sub>8</sub> +( <i>S</i> )-TFAE <sup>a</sup>	—	2.88, 2.86, 2.79, 2.78	—
( $\pm$ )- <b>5</b>	Toluene- <i>d</i> <sub>8</sub>	—	3.08 and 3.02	—
	Toluene- <i>d</i> <sub>8</sub> +( <i>S</i> )-TFAE <sup>a</sup>	—	3.08, 3.06, 2.99, 2.98	—

<sup>a</sup> 1:6 equiv of (*S*)-TFAE were used.

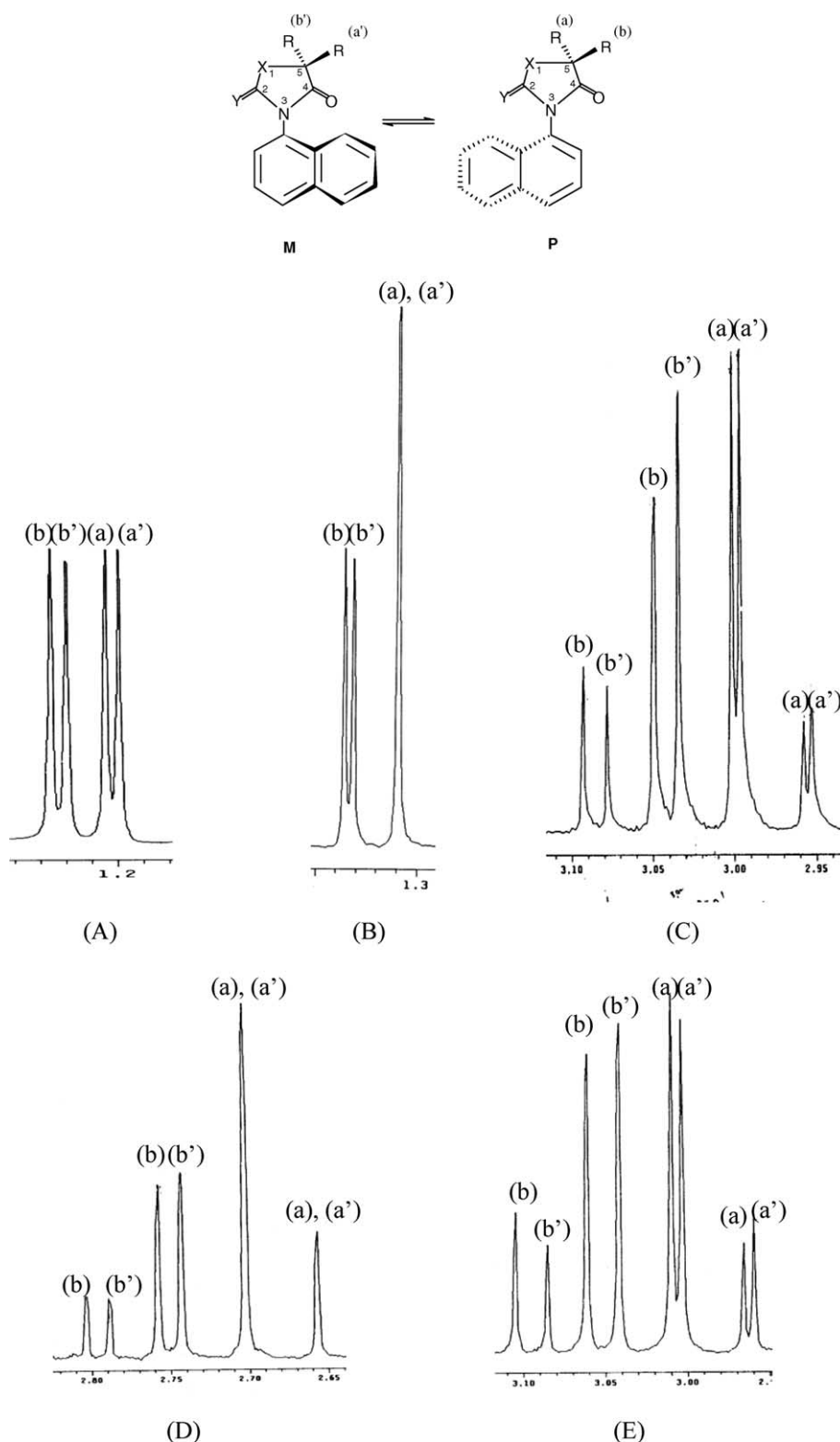


**Figure 1.** The  $^1\text{H}$  NMR spectra of the compounds ( $\pm$ )-1–5 taken in the presence of 6 equiv of (*S*)-TFAE in toluene- $d_8$ , A = ( $\pm$ )-1, B = ( $\pm$ )-2, C = ( $\pm$ )-3, D = ( $\pm$ )-4 and E = ( $\pm$ )-5.

### 2.3. Determination of absolute stereochemistry

The resolution of the enantiomeric resonances of 5,5-dimethyl-3-(*o*-aryl)-2,4-oxazolidinones was accomplished through the interaction of the enantiomers

with the chiral auxiliary (*S*)-TFAE.<sup>6</sup> For 5,5-dimethyl-3-(*o*-iodophenyl)-2,4-oxazolidinone studied in previous work,<sup>6</sup> four singlets corresponding to the C-5 methyl groups of **M** and **P** rotational isomers could be distinguished by  $^1\text{H}$  NMR in the presence of (*S*)-TFAE.

For this compound the chemical shift difference between the diastereotopic C-5 methyl protons (0.19 ppm in  $C_6D_6$ ) did not change with the addition of (*S*)-TFAE while cooling a toluene- $d_8$  solution in the NMR probe from 30 to  $-70$  °C did not result in a significant difference in chemical shifts. Contrary to this, it was observed for compound ( $\pm$ )-**1** that the chemical shift difference between the diastereotopic C-5 methyl protons were found to be slightly different in the absence (0.040 ppm, in toluene- $d_8$ ) and presence (0.046 ppm, in toluene- $d_8$ ) of (*S*)-TFAE. Moreover the  $^1H$  NMR of this compound in toluene- $d_8$ , unlike the 5,5-dimethyl-3-(*o*-iodophenyl)-2,4-oxazolidinedione, showed a strong temperature dependence,<sup>8,9</sup> in the 30 to  $-70$  °C range (Fig. 2). We presume that this may arise from the existence of a naphthyl group and hence  $\pi$  stacking. Therefore to relate these results to a solvation model we studied sterically congested, axially chiral heterocyclic compounds (Scheme 1) bearing a naphthyl ring that would facilitate studies of intermolecular interactions between stacked aromatic groups. We surmise that the stacking propensity of a naphthyl ring with an anthryl group of (*S*)-TFAE would be higher than that of the *o*-iodo substituted phenyl ring due to the high surface area of naphthyl.<sup>10,11</sup>

Among these compounds ( $\pm$ )-**1–5** the enantiomers of 2,4-oxazolidinedione ( $\pm$ )-**1** and **3** and 2,4-thiazolidinedione ( $\pm$ )-**5** derivatives could be differentiated by  $^1H$  NMR spectroscopy in the presence of (*S*)-TFAE (Fig. 1). The better resolution of the 2,4-oxazolidinediones ( $\pm$ )-**1** and

**3** led us to consider that the origin of this resolution was much the same as it was in our previous work on 5,5-dimethyl-3-(*o*-aryl)-2,4-oxazolidinediones. However on lowering the temperature, the C-5 methyl and C-5 methylene  $^1H$  NMR signals of the complexed enantiomers of the  $\alpha$ -naphthyl derivatives showed a different shielding behaviour, as will be discussed below, from what had been observed for the *o*-iodophenyl derivative. It is also interesting to note that the  $^1H$  NMR spectra of all comparable signals through the series showed close similarities. The C-5 methyl groups of compounds ( $\pm$ )-**1** and ( $\pm$ )-**2** were shielded in the same way upon cooling while the signals of the C-5 methylene for compounds ( $\pm$ )-**3**, **4** and **5** were shielded in a similar way on cooling. The fact that the temperature dependence of the C-5 methylene signals for compounds ( $\pm$ )-**4** and ( $\pm$ )-**5** was similar with that of compound ( $\pm$ )-**3** led us think that all of these compounds could have the same solvation model, although the enantiomers of ( $\pm$ )-**2** and ( $\pm$ )-**4** could not be completely resolved.

By considering these results it can be said that the solvation model for all of these compounds ( $\pm$ )-**1–5** should be the same within the series and is very similar to that proposed for 5,5-dimethyl-3-(*o*-aryl)-2,4-oxazolidinediones.<sup>6</sup> However, there must be a difference from the previously proposed model to account for the different temperature dependence of the signals.

In order to obtain a solvation model for our compounds, all  $^1H$  NMR signals of pure (*S*)-TFAE and each

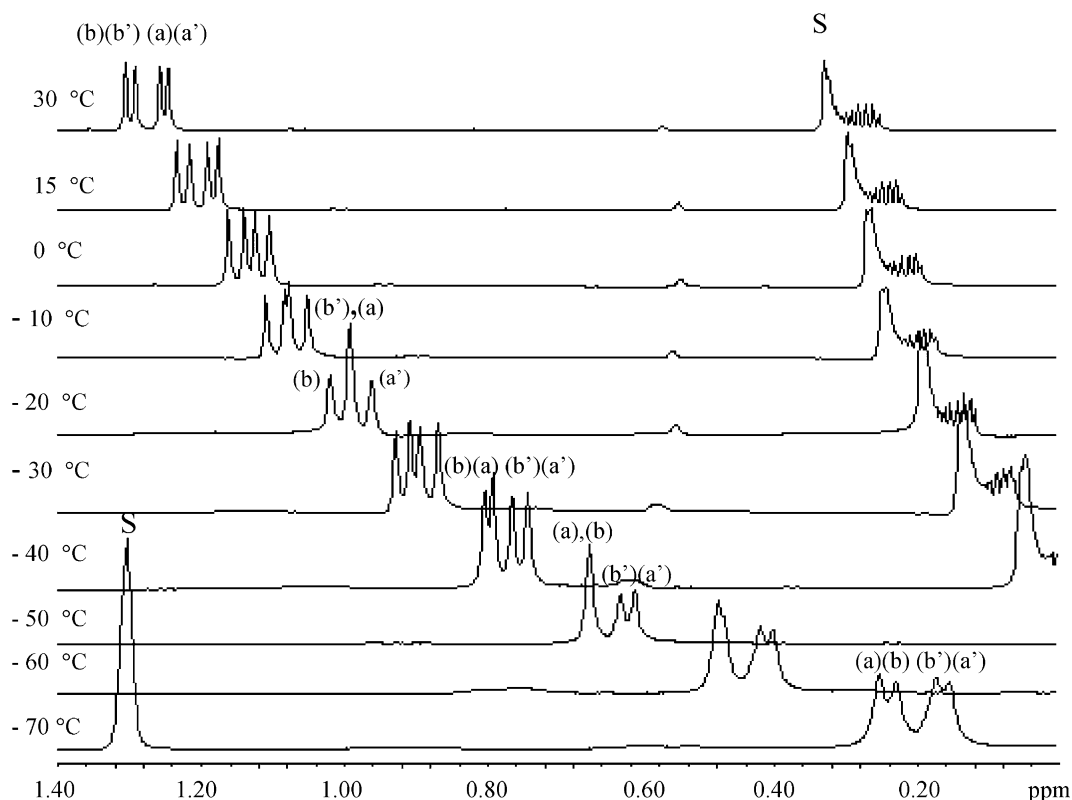


**Figure 2.** The temperature dependence of the  $^1H$  NMR signals of the methyl groups on C-5 of the compound ( $\pm$ )-**1** upon cooling from 30 to  $-70$  °C, S: solvent.

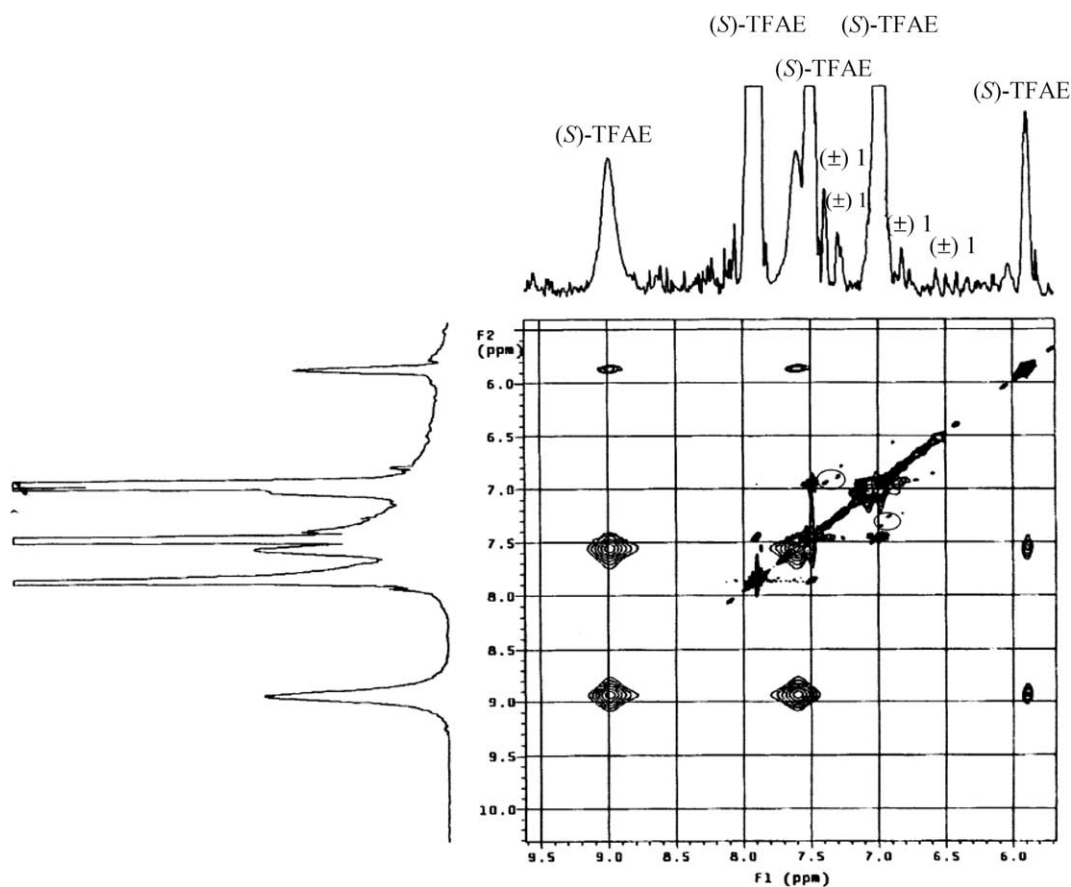


**Figure 3.** The NOESY spectrum of compound ( $\pm$ )-**1** taken in the presence of (*S*)-TFAE. The cross-peaks between the naphthyl and the anthryl rings are shown in circles.

of the racemates were compared with those of the diastereomeric association complex. It was observed that for all of the signals of complexed (*S*)-TFAE and the enantiomers, with the exception of the hydroxyl group of (*S*)-TFAE, were shielded with respect to the corresponding pure compounds and these observed upfield shifts and the downfield shift increased with decreasing temperature.<sup>9</sup>

The downfield shift observed for the hydroxyl proton was thought to result from hydrogen bonding with racemates.<sup>11</sup> The upfield changes in chemical shifts observed for the aromatic naphthyl and anthryl groups may arise from ring current effects and suggests a face-to-face  $\pi$  stacked geometry (Fig. 3).<sup>10,12</sup> Also consistent with the face-to-face  $\pi$  stacking, cross-peaks between some of the protons of naphthyl and anthryl ring of (*S*)-TFAE were observed in the NOESY spectrum (Fig. 3). The  $\pi$  stacking tendency of the naphthyl substituent in a  $\pi$ - $\pi$  interaction as a  $\pi$ -base,<sup>2</sup> was thought to be higher,<sup>10,11</sup> and hence these compounds ( $\pm$ )-**1–5** would form tighter complexes with (*S*)-TFAE than that of the *o*-iodo substituted phenyl ring. The change in the chemical shift difference of the diastereotopic C-5 protons of compound ( $\pm$ )-**1** from 0.040 to 0.046 ppm upon complex formation, might be further indication for an increase in anisotropic shielding effect as a result of enhanced  $\pi$  stacking between the aromatics. In order to find out whether the observed shielding was influenced by the effect of

the solvent used or by enforced  $\pi$ - $\pi$  interaction, the toluene-*d*<sub>8</sub> solution of compound ( $\pm$ )-**1** was cooled to 0 °C in the absence of (*S*)-TFAE. The fact that none of the protons of compound ( $\pm$ )-**1** indicated any shielding effect on cooling to 0 °C revealed the enhanced  $\pi$ - $\pi$  interaction between the anthryl group of the (*S*)-TFAE and the naphthyl substituent of the enantiomers.

In our previous work carried out for diastereomeric (*5S*)-methyl-3(*o*-aryl)-2,4-oxazolidinediones it was found that the naphthyl substituent exerted a similar shielding effect as the iodine<sup>13</sup> on the C-5 methyl group, which is on the same side with the naphthyl or iodine. Similarly, the enantiomers of compounds ( $\pm$ )-**1–5** studied in the absence of (*S*)-TFAE could be differentiated on the NMR time scale via the diastereotopic groups on C-5 (a–b or a'–b')<sup>†</sup> (Fig. 1) depending on the position of naphthyl substituent. In the presence of (*S*)-TFAE however, the discrimination of the enantiotopic groups (a–a' and b–b') was also possible.

For the **M** and **P** conformations the hydroxyl group of (*S*)-TFAE formed a hydrogen bond with the carbonyl or thiocarbonyl groups; the carbonyl hydrogen of

<sup>†</sup>Notations a, b, a', b' refer to the C-5 methyl protons for the compounds ( $\pm$ )-**1–2** and the C-5 methylene protons for the compounds ( $\pm$ )-**3–5**.

(*S*)-TFAE involved in hydrogen bonding with the oxygen or sulfur atoms of the heterocycle formed a chelate-like structure and the anthryl group of (*S*)-TFAE formed a  $\pi$ - $\pi$  interaction with the naphthyl substituent of the enantiomers (Fig. 4, models A and C). As can be seen in Figure 4, during the interaction of compound ( $\pm$ )-1 with (*S*)-TFAE, two more, different, solvation models (B and D in Fig. 4) are possible for both conformers. In our basic models (A and C in Fig. 4) (*S*)-TFAE forms a chelate via a hydrogen bond between the C–H proton of the (*S*)-TFAE and the ring oxygen and a hydrogen bond between the –OH group of the (*S*)-TFAE and the –C=O on C-2. However, a  $\pi$ - $\pi$  interaction would also be possible between the anthryl and the naphthyl rings, thus destroying the chelate structure without cleavage of the hydrogen bonding with the C-2 carbonyl group. In these models (B and D in Fig. 4),

anthryl<sub>2</sub> cannot approach the naphthyl due to the presence of anthryl<sub>3</sub> and the weak basicity of the naphthyl. Therefore, either carbonyl hydrogen bonding (A and C) or  $\pi$ - $\pi$  interaction (B and D) should be preferred at a given time, one being more populated than the other. The models B and D were thought to be less populated than the models A and C since they have less interactions. Compared to model D, model B would be even less populated due to the weaker  $\pi$ - $\pi$  interaction. Therefore, it was thought that model B may have little or no effect on the observed chemical shifts. The observed <sup>1</sup>H NMR signals should be consistent with the time-averaged structure of these solvates.

In order to assign the pairs (a–b or a'–b') corresponding to the signals of the diastereotopic methyl or methylene protons, the second eluted enantiomers of ( $\pm$ )-2 and

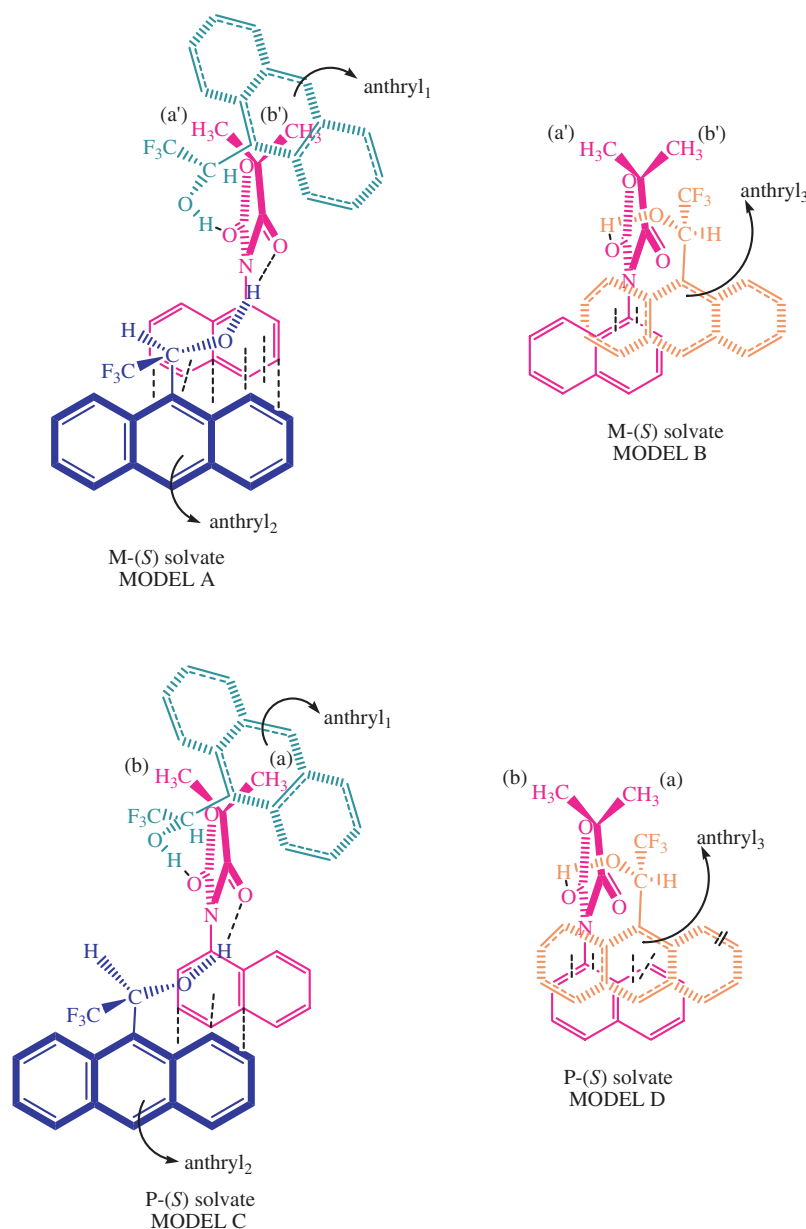


Figure 4. The proposed solvation models for the M and the P enantiomers of ( $\pm$ )-1.

(±)-**4** resolved by HPLC on a Chiralpak AD-H was added into a toluene-*d*<sub>8</sub> solution containing racemic compound and (*S*)-TFAE. With the NMR spectrum, it was observed that the intensity of the signals belonging to this enantiomer, which were the more shielded of the C-5 methyl or methylene proton signals (Fig. 1B and D) increased. For compounds (±)-**3**, **4** and **5** the splitting patterns of the AB spectra enabled us to distinguish between the signals of **M** and **P** conformers.

The assignments of the four peaks to the four methyl groups (Figs. 1 and 4) as a, a', b, b' has been done in the following way: Protons (a) and (a') were both affected by the shielding zone of the naphthyl group, giving the signals in the upfield region compared to (b), (b'). Additionally, proton (a) of the **P** conformer was affected by the shielding zone of anthryl<sub>3</sub> (Fig. 4, model D) and anthryl<sub>1</sub> (Fig. 4, model C), whereas the proton (a') was shielded by anthryl<sub>2</sub> (Fig. 4, model A). Since anthryl<sub>2</sub> was closer to proton (a') and the **M** conformation could form a tighter complex,<sup>14</sup> this proton should be more shielded with respect to proton (a) of the **P** conformer.

Protons (b) and (b') were not affected by the naphthyl (Fig. 4). Proton (b) spends some of the time in the shielding zone of the anthryl<sub>2</sub> (Fig. 4, model C), some of the time not (Fig. 4, model D), whereas the proton (b') was always affected by anthryl<sub>1</sub> (Fig. 4, model A). Since (b') experiences a stronger shielding effect than proton (b) of the **P** conformer it appeared more shielded than b. Therefore it can be argued that for all the compounds studied (±)-**1–5**, in the presence of (*S*)-TFAE the more deshielded of the diastereotopic C-5 methyl and the methylene protons (Fig. 1) can be assigned to the complexed **P** conformer and the more shielded to complexed **M** (Fig. 1). Thus, the second eluted enantiomers of (±)-**2** and (±)-**4** have been assigned to **M** conformation.

The model also accounts for the difference in chemical shifts between the a and a' (upfield, 0.01 ppm) and the b–b' (downfield, 0.02 ppm) pairs (Fig. 1C), which was absent for *o*-iodo derivative.<sup>6</sup> Since the a and a' protons were subjected to similar anisotropy effects, the chemical shift difference between them was smaller than that of b and b'.

The non-resolved (a) and (a') protons of compounds (±)-**2** and (±)-**4** (Fig. 1) can be explained on the basis of the ring size of the chelate structure formed between the (*S*)-TFAE and the ring oxygen or sulfur and the C=O or C=S groups of the heterocycle (Fig. 4), changing the geometry of the ring formed on chelation. In compounds (±)-**2** and (±)-**4**, although anthryl<sub>1</sub> was closer to the proton (a) than (±)-**1**, **3** and **5**, anthryl<sub>3</sub> was far away from it (model D). This causes a similar shielding effect on protons (a) and (a'), giving the same chemical shift values for these compounds.

On cooling, it was observed that the upfield chemical shift differences of the <sup>1</sup>H NMR signals of the C-5 methyl groups of the compounds (±)-**1** and (±)-**2**

increased in the following order: (b') > (b) > (a') > (a)<sup>‡</sup> (Fig. 2). However the signals of C-5 methylene protons of compounds (±)-**3**, (±)-**4** and (±)-**5** had a shift pattern that was in the following order: (b') > (a') > (a) > (b). The observed chemical shift behaviour on cooling can be explained on the basis of the proposed solvation model (Fig. 4). The fact that the aromatic protons of the naphthyl and the anthryl rings were more shielded and the hydroxyl proton was more deshielded compared to the values at 30 °C, pointed that all of the intermolecular interactions were getting stronger upon cooling. This result may be attributed to the slower rotation of the molecules at lower temperatures. The conformation might even have been frozen at –70 °C. For example, the aromatic groups of the enantiomers and (*S*)-TFAE could be positioned parallel to each other enhancing the intermolecular interactions. In compounds (±)-**1** and (±)-**2** as the temperature was lowered, the change in the chemical shift values of proton (b') of the **M** conformer was the most affected one and was strongly shielded. Based on our model this proton was already strongly affected by an average anisotropy of the anthryl<sub>1</sub> at 30 °C where its rotation was fast around C<sub>sp<sup>2</sup></sub>–C<sub>sp<sup>3</sup></sub> single bond of (*S*)-TFAE. However, decreasing the temperature made this rotation slower, making the anthryl<sub>1</sub> adopt a conformation where the hydroxyl group and the carbonyl hydrogen were aligned on the same side and –CF<sub>3</sub> positioned nearly orthogonal to the plane of the anthryl group.<sup>15</sup> In this conformation the anthryl<sub>1</sub> would be closer to the proton (b') thus shielding it more.

At 30 °C, both of the solvation models (C and D in Fig. 4) are possible for the **P** conformer, with model C being more populated. Proton (b) was only affected by the anisotropy of anthryl<sub>2</sub> during solvation C, as shown in Figure 4. Therefore, its shielding was only explained on the basis of Model C. Upon cooling the change in the solvation model from D to C (Fig. 4) the anisotropy effect on this proton increased, making it more shielded.

In model A there was a strong π–π interaction between the aromatic rings, affecting proton (a'). This intermolecular interaction became stronger upon cooling, making this proton more shielded.

Proton (a) was affected by the average shielding effect of both anthryl<sub>1</sub> and anthryl<sub>2</sub> at 30 °C. However, on cooling the **P** enantiomer may prefer the model C where the proton (a) was only affected by anthryl<sub>1</sub>. This proton although can be expected to be less shielded due to the same reason noted for proton (b), shielding by the anthryl<sub>1</sub> had a compensating effect and thus the chemical shift of this proton did not change much on cooling.

Regarding these results it can be said that the diastereotopic methyl signals of the **M** conformer, forming a tighter complex with (*S*)-TFAE, was shielded more compared to that of the **P** conformer. These results

<sup>‡</sup>For compound (±) **2** and (±) **4** the chemical shift values of (a) and (a') were the same.

are also consistent with what we observed for 5,5-dimethyl-3-(*o*-iodophenyl)-2,4-oxazolidinedione on cooling. For this compound, although the chemical shift of the signals did not change significantly, the signals of the **P** conformer, which formed a tighter complex with (*S*)-TFAE were the most shielded ones upon cooling.

The different shift pattern observed for the compounds ( $\pm$ )-**3–5** upon cooling may arise from the difference in the van der Waals radii of C-5 methyl and methylene protons. Since methyl protons are exposed into space more, these protons may experience a different anisotropic effect. Even if a different shift pattern was observed for these compounds on cooling, the diastereotopic methyl signals of the **M** conformer (a'-b') was the most shielded ones as observed in the compounds ( $\pm$ )-**1, 2**.

#### 2.4. Activation barriers to hindered rotation

Activation barriers to the hindered rotation of the compounds studied were determined either by temperature dependent NMR or by enantioresolution on a chiral sorbent via HPLC. If the barrier to the restricted rotation about C<sub>sp<sup>2</sup></sub>-N<sub>sp<sup>2</sup></sub> chiral axis is sufficiently high, the separation of enantiomeric rotational isomers would be possible by HPLC.

Dynamic NMR studies of all the compounds, except for compound ( $\pm$ )-**1**, indicated no coalescence for the diastereotopic protons up to 110 °C due to the high activation barrier for restricted rotation. Therefore, thermal racemization after micropreparative enrichment of these enantiomers was applied to calculate the barriers. Enan-

tioresolution of the racemic mixtures was done on Chiralpak AD-H column packed with amylose tris-(3,5-dimethyl)-carbamate as chiral stationary phase and thermal racemization process was followed by UV at 254 nm. To obtain a better resolution of the enantiomers, all chromatographic separations were conducted at  $7 \pm 2$  °C. The same procedure described in our previous work,<sup>6</sup> was followed for thermal racemization. The activation parameters of compounds ( $\pm$ )-**2**, ( $\pm$ )-**3**, ( $\pm$ )-**4** and ( $\pm$ )-**5** are listed in Table 2 and data pertinent to the chromatographic separations of the enantiomers on Chiralpak AD-H are shown in Table 3.

Activation parameters of ( $\pm$ )-**1** were found by dynamic NMR spectroscopy. The two singlets of the diastereotopic C-5 methyl protons that were distinguishable at 30 °C coalesced into one peak at higher temperatures due to the fast rotation. The kinetic data of the interconversion process were determined by the Eyring equation,<sup>16</sup> and it was apparent that the barrier (85.01 kJ/mol in DMSO-*d*<sub>6</sub>, Table 2) was not high enough to allow the resolution of compound ( $\pm$ )-**1** into the enantiomers on Chiralpak AD-H.

The barriers of 2,4-oxazolidinediones ( $\pm$ )-**1** and ( $\pm$ )-**3** (Y = O, Scheme 1) and 2,4-thiazolidinedione ( $\pm$ )-**5** (Y = O) derivatives were found to be lower than that of the rhodanine ( $\pm$ )-**4** (Y = S) and 2-thioxo-4-oxazolidinone (compound ( $\pm$ )-**2**, Y = S) derivatives. This difference was interpreted by means of the higher standard bond length of the C=S double bond (1.71 Å) than that of the C=O (1.22 Å) and the larger van der Waals radius of sulfur (1.85 Å) than that of the oxygen atom (1.40 Å). In compounds ( $\pm$ )-**2** and ( $\pm$ )-**4** the repulsion between

**Table 2.** The kinetic and thermodynamic data for the interconversion process shown in Scheme 1

Compound no.	Solvent	<i>T</i> , K	<i>k</i> , s <sup>-1</sup>	$\Delta G^\ddagger$ , kJ/mol
( $\pm$ )- <b>1</b>	DMSO- <i>d</i> <sub>6</sub>	398 <sup>a</sup>	54.52 <sup>b</sup>	85.01 ± 0.05 <sup>c</sup>
	Toluene- <i>d</i> <sub>8</sub>	378 <sup>a</sup>	36.62 <sup>b</sup>	81.83 ± 0.05 <sup>c</sup>
( $\pm$ )- <b>2</b>	Ethanol/hexane (20%:80%, v/v)	333 <sup>d</sup>	4 × 10 <sup>-5</sup> <sup>e</sup>	109.9 ± 0.07 <sup>f</sup>
( $\pm$ )- <b>3</b>	Ethanol/hexane (60%:40%, v/v)	313 <sup>d</sup>	3 × 10 <sup>-5</sup> <sup>e</sup>	103.8 ± 0.07 <sup>f</sup>
( $\pm$ )- <b>4</b>	Ethanol/hexane (50%:50%, v/v)	351 <sup>d</sup>	2 × 10 <sup>-4</sup> <sup>e</sup>	111.3 ± 0.07 <sup>f</sup>
( $\pm$ )- <b>5</b>	Ethanol/hexane (70%:30%, v/v)	323 <sup>d</sup>	5 × 10 <sup>-5</sup> <sup>e</sup>	105.9 ± 0.07 <sup>f</sup>

<sup>a</sup> The coalescence temperature.

<sup>b</sup> Rate constant at coalescence temperature.

<sup>c</sup> Free energy of activation determined by 400 MHz NMR instrument.

<sup>d</sup> The temperature at which the thermal racemization has been done.

<sup>e</sup> The rate constant of interconversion.

<sup>f</sup> Free energy of activation determined by HPLC.

**Table 3.** Chromatographic parameters for the separation of enantiomers by HPLC on Chiralpak AD-H at  $7 \pm 2$  °C

Compound no.	Eluent composition	Retention times, <i>t</i> <sub>1</sub> , <i>t</i> <sub>2</sub> , min	Capacity factors, <i>k</i> <sub>1</sub> , <i>k</i> <sub>2</sub>	Selectivity, $\alpha$	Flow rate, ml/min
( $\pm$ )- <b>2</b>	Ethanol/hexane (20%:80%, v/v)	12.96	1.23	1.30	0.5
		15.08	1.60		
( $\pm$ )- <b>3</b>	Ethanol/hexane (60%:40%, v/v)	19.71	2.40	1.79	0.5
		30.78	4.31		
( $\pm$ )- <b>4</b>	Ethanol/hexane (50%:50%, v/v)	16.56	1.86	1.58	0.5
		22.86	2.94		
( $\pm$ )- <b>5</b>	Ethanol/hexane (70%:30%, v/v)	17.54	2.02	1.26	0.5
		20.54	2.54		



the thiocarbonyl sulfur atom and the peri hydrogen of the naphthyl group in the transition state serves as a steric impediment to the enantiomer interconversion and makes the passage of the peri hydrogen more difficult, which in turn, increases the barrier to hindered rotation.

Compound ( $\pm$ )-**5** ( $X = S$ ) showed a barrier greater than compounds ( $\pm$ )-**1** and ( $\pm$ )-**3** ( $X = O$ ). This difference can be explained by considering the standard bond length of C–S (182 pm) and C–O (143 pm) single bonds as has been observed before.<sup>17</sup> Owing to the larger bond length of C–S, the C-2 carbonyl group of compound ( $\pm$ )-**5** is closer to the peri hydrogen of the naphthyl substituent in the transition state, giving rise to an enantiomeric pair of **M** and **P** atropisomers with higher activation barriers for interconversion.

Comparison of the energy barriers of compounds ( $\pm$ )-**1** and ( $\pm$ )-**3** revealed the influence of the solvent used (Table 2). Compound ( $\pm$ )-**3** unexpectedly exerted a higher barrier than compound ( $\pm$ )-**1** although the X and Y groups were the same (Scheme 1). This result can be attributed to the solvent effect,<sup>13</sup> of ethanol that may form hydrogen bonds with the C=O groups at the 2- and 4-positions and thus make the rotation around the C<sub>sp<sup>2</sup></sub>–N<sub>sp<sup>2</sup></sub> bond more hindered.

### 3. Conclusion

The enantiotopic protons of naphthyl compounds ( $\pm$ )-**1–5** could be resolved in the presence of the chiral auxiliary (*S*)-TFAE. The proposed model between the compounds and the chiral auxiliary, which emphasized  $\pi$ – $\pi$  interactions between the naphthyl and anthryl groups as well as the hydrogen bonding interactions enabled the assignment of the resolved peaks to the **M** and **P** conformations. The strong temperature dependence of the spectra of the diastereomeric complexes originated from the adoption of different solvation models at lower temperatures of the **M** and **P** conformers. Thus, at 30 °C or lower for the **M** conformation, the most dominant model was the model A (Fig. 4) while for the **P** was the model C (Fig. 4). The population of model C increased even more on cooling upon the change from solvation model D to C.

The assignment of the <sup>1</sup>H NMR signals of the **M** and **P** conformations also enabled us to relate the elution order in HPLC on Chiralpak AD-H to the absolute conformations for the compounds ( $\pm$ )-**2** and ( $\pm$ )-**4**. The second eluted enantiomer had the **M** conformation on chiral AD-H column for both compounds.

The activation barrier for 5,5-dimethyl-3-( $\alpha$ -naphthyl)-2,4-oxazolinedione was determined as 85.01 kJ/mol in DMSO-*d*<sub>8</sub> by temperature dependent NMR. The enantiomers of 5,5-dimethyl-3-( $\alpha$ -naphthyl)-2-thioxo-4-oxazolinedione, 5,5-dimethyl-3-( $\alpha$ -naphthyl)-2,4-oxazolinedione, 3-( $\alpha$ -naphthyl)-rhodanine and 3-( $\alpha$ -naphthyl)-2,4-thiazolinedione were resolved micro-preparatively on Chiralpak AD-H. The thermal racemization of the enriched enantiomer was followed to

obtain the barriers to rotation, which were found as 109.9, 103.8, 111.3 and 105.9 kJ/mol, respectively. The difference in activation barriers resulted from the higher bond length of the C=S double bond than that of C=O, and the larger van der Waals radius of the sulfur atom than that of the oxygen atom. The solvent effect of ethanol caused an increase in activation barriers by forming hydrogen bonds with the oxygen atom of C=O groups making the rotation more hindered.

## 4. Experimental

<sup>1</sup>H and <sup>13</sup>C NMR spectra of all compounds were recorded on a Varian-Mercury VX-400 MHz-BB (30 °C). Chromatographic analyses were done using Cecil 1100 pump ( $P = 3$ – $3.5$  MPa), a Rheodyne, 7125 injector mode with a 20  $\mu$ l Sample loop, a Cecil UV monitor (240 nm) and an integrating recorder. The chiral column used was commercially available Chiralpak AD-H (4.6 mm I.D.  $\times$  250 mm *L*, 5  $\mu$ m, Daicel, Tokyo, Japan). Thermohypersil-Keystone column pocket was used for the temperature control of the Chiralpak AD-H column. Elemental analyses were performed on Carlo Erba 1106. Melting points were recorded using Electrothermal 9100 melting point apparatus.

### 4.1. General procedure for the preparation of the compounds studied ( $\pm$ )-**1–5**

The compounds were synthesized by the reaction of 0.02–0.03 mol of  $\alpha$ -naphthyl isocyanate or  $\alpha$ -naphthyl isothiocyanate and an equimolar amount of the corresponding ethyl esters (ethyl glycolate, ethylthioglycolate or ethyl  $\alpha$ -hydroxy isobutyrate) in the presence of sodium metal in toluene.

In a 100-ml three-necked flask, fitted with a thermometer and a reflux condenser,  $\alpha$ -naphthyl isocyanate or  $\alpha$ -naphthyl isothiocyanate and corresponding ethyl esters were mixed in toluene. Sodium metal in small pieces was added prior to heating. The mixture was heated for 10 h at about 80 °C after which the temperature was increased to 100–110 °C for 1 h.<sup>§</sup> At the end of the reflux process, crude products were obtained. After dissolving in ethanol, the compounds separated as crystals. The compounds were further purified by recrystallization from ethanol and identified based on their <sup>1</sup>H NMR spectra and elemental analyses.

**4.1.1. Synthesis of 5,5-dimethyl-3-( $\alpha$ -naphthyl)-2,4-oxazolinedione, ( $\pm$ )-**1**.** Compound ( $\pm$ )-**1** was prepared according to the general procedure using 0.03 mol  $\alpha$ -naphthyl isocyanate, 0.03 mol ethyl  $\alpha$ -hydroxy isobutyrate, 0.003 mol sodium metal and 25 ml toluene. Yield: 5.98 g, 78%. Melting point: 142–143 °C. <sup>1</sup>H NMR (400 MHz) data in CDCl<sub>3</sub>: Diastereotopic methyl protons at C-5:  $\delta = 1.77$  ppm (s, 3H), 1.69 ppm (s, 3H). Aromatic protons:  $\delta = 7.9$ – $7.16$  ppm (m, 7H). <sup>13</sup>C NMR data in CDCl<sub>3</sub>: Carbonyl carbons in the heterocyclic

<sup>§</sup>The reaction mixture was refluxed for 7 h for ( $\pm$ )-**2**.

ring: 176.6, 153.7 ppm. Aromatic carbons: 134–121 ppm. Methine carbon (C-5): 84 ppm. Diastereotopic methyl carbons at C-5: 25 and 24 ppm. Elemental analysis data: Calculated for  $C_{15}H_{13}NO_3$ : C, 70.59; H, 5.09; N, 5.49. Found: C, 69.96; H, 4.81; N, 5.22.

**4.1.2. Synthesis of 5,5-dimethyl-3-( $\alpha$ -naphthyl)-2-thioxo-4-oxazolidinedione, ( $\pm$ )-2.** Compound ( $\pm$ )-2 was prepared according to the general procedure using 0.025 mol  $\alpha$ -naphthyl isothiocyanate, 0.025 mol ethyl  $\alpha$ -hydroxy isobutyrate, 0.0025 mol sodium metal and 25 ml toluene. Yield: 1.7 g, 24%. Melting point: 155 °C.  $^1H$  NMR (400 MHz) data in toluene- $d_8$ : Diastereotopic methyl protons at C-5:  $\delta = 1.27$  ppm (s, 3H), 1.22 ppm (s, 3H), Aromatic protons:  $\delta = 7.60$ –6.90 ppm (m, 7H).  $^{13}C$  NMR data in  $CDCl_3$ : Carbonyl carbons in the heterocyclic ring: 194, 181 ppm. Aromatic carbons: 142–126 ppm. Methine carbon (C-5): 92 ppm. Diastereotopic methyl carbons at C-5: 29 and 28 ppm. Elemental analysis data: Calculated for  $C_{15}H_{13}NO_2S$ : C, 66.42; H, 4.79; N, 5.17; S, 11.80. Found: C, 65.68; H, 4.37; N, 4.95; S, 10.67.

**4.1.3. Synthesis of 3-( $\alpha$ -naphthyl)-2,4-oxazolidinedione, ( $\pm$ )-3.** Compound ( $\pm$ )-3 was prepared according to the general procedure using 0.02 mol  $\alpha$ -naphthyl isocyanate, 0.02 mol ethyl glycolate, 0.002 mol sodium metal and 15 ml toluene. Yield: 0.78 g, 17.30%. Melting point: 152–154 °C.  $^1H$  NMR (400 MHz) data in  $CDCl_3$ :  $\delta_A = 4.56$  and  $\delta_B = 4.52$  (AB,  $J_{AB} = 5$  Hz, 2H), Aromatic protons:  $\delta = 7.50$ –8.10 (m, 7H).  $^{13}C$  NMR data in  $CDCl_3$ : Carbonyl carbons in the heterocyclic ring: 167, 151 ppm. Aromatic carbons: 134–118 ppm, Methylene carbon (C-5): 63 ppm.

**4.1.4. Synthesis of 3-( $\alpha$ -naphthyl)-rhodanine, ( $\pm$ )-4.** Compound ( $\pm$ )-4 was prepared according to the general procedure using 0.023 mol  $\alpha$ -naphthyl isothiocyanate, 0.023 mol ethylthioglycolate, 0.0023 mol sodium metal and 25 ml toluene. Yield: 2.4 g, 41%. Melting point: 171–172 °C.  $^1H$  NMR (400 MHz) data in  $CDCl_3$ : Diastereotopic methyl protons at C-5:  $\delta_A = 4.38$  and  $\delta_B = 4.30$  (AB,  $J_{AB} = 5$  Hz, 2H). Aromatic protons:  $\delta = 8.01$ –7.25 (m, 7H).  $^{13}C$  NMR data in  $CDCl_3$ : Carbonyl carbons in the heterocyclic ring: 200, 173 ppm. Aromatic carbons: 134–119 ppm, Methylene carbon (C-5): 37 ppm. Elemental analysis data: Calculated for  $C_{13}H_9NOS_2$ : C, 60.23; H, 3.47; N, 5.40; S, 24.71. Found: C, 60.13; H, 3.35; N, 5.20; S, 25.08.

**4.1.5. Synthesis of 3-( $\alpha$ -naphthyl)-2,4-thiazolidinedione, ( $\pm$ )-5.** Compound ( $\pm$ )-5 was prepared according to the general procedure using 0.02 mol  $\alpha$ -naphthyl isocyanate,

0.02 mol ethylthioglycolate, 0.002 mol sodium metal and 25 ml toluene. Yield: 2.07 g, 42%. Melting point: 158 °C.  $^1H$  NMR (400 MHz) data in  $CDCl_3$ : Diastereotopic methyl protons at C-5:  $\delta_A = 4.31$  and  $\delta_B = 4.27$  (AB,  $J_{AB} = 5$  Hz, 2H), Aromatic protons:  $\delta = 7.91$ –7.18 (m, 7H).  $^{13}C$  NMR data in  $CDCl_3$ : Carbonyl carbons in the heterocyclic ring: 170.9, 170.8 ppm, Aromatic carbons: 135–122 ppm, Methylene carbon (C-5): 35 ppm. Elemental analysis data: Calculated for  $C_{13}H_9NO_2S$ : C, 64.19; H, 3.70; N, 5.76; S, 13.17. Found: C, 63.11; H, 3.63; N, 5.69; S, 13.46.

### Acknowledgement

This project has been supported by Boğaziçi University research fund (BAP) with project number 05B501.

### References

- Evans, D. A.; Chapman, K. T.; Hung, D. T.; Kawaguchi, A. T. *Angew. Chem., Int. Ed. Engl.* **1987**, *26*, 1184.
- Pirkle, W. H.; Pochapsky, T. C. *J. Am. Chem. Soc.* **1987**, *109*, 5975–5982.
- Cochran, J. E.; Parrot, T. J.; Whitlock, B. H.; Whitlock, H. W. *J. Am. Chem. Soc.* **1982**, *114*, 2269–2270.
- Pirkle, W. H.; Sikkenga, D. L. *J. Org. Chem.* **1977**, *42*, 1370–1374.
- Jullian, J.-C.; Franck, X.; Latypov, S.; Hocquemiller, R.; Figadère, B. *Tetrahedron: Asymmetry* **2003**, *14*, 963–966.
- Demir Ordu, Ö.; Doğan, İ. *Tetrahedron: Asymmetry* **2004**, *15*, 925–933.
- Doğan, İ.; Burgemeister, T.; İçli, S.; Mannschreck, A. *Tetrahedron* **1992**, *48*, 7157–7164.
- Pirkle, W. H.; Beare, S. D.; Muntz, R. L. *Tetrahedron Lett.* **1974**, *26*, 2295–2298.
- Hanna, G. M.; Evans, F. E. *J. Pharm. Biomed. Anal.* **2000**, *24*, 189–196.
- Guckian, K. M.; Schweitzer, B. A.; Ren, R. X.-F.; Sheils, C. J.; Tahmassebi, D. C.; Kool, E. T. *J. Am. Chem. Soc.* **2000**, *122*, 2213–2222.
- Rotello, V. M.; Viani, E. A.; Deslongchamps, G.; Murray, B. A.; Rebek, J. *J. Am. Chem. Soc.* **1993**, *115*, 797–798.
- Muehldorf, A. V.; Engen, D. V.; Warner, J. C.; Hamilton, A. D. *J. Am. Chem. Soc.* **1988**, *110*, 6561–6562.
- Demir, Ö.; Doğan, İ. *Chirality* **2003**, *15*, 242–250.
- Beaufour, M.; Merelli, B.; Menguy, L.; Cherton, J. C. *Chirality* **2003**, *15*, 382–390.
- Pirkle, W. H.; Finn, J. M. *J. Org. Chem.* **1981**, *46*, 2935–2938.
- Alberty, R. A.; Silbey, R. J. *Physical Chemistry*; Wiley: New York, 1992.
- Doğan, İ.; Pustet, N.; Mannschreck, A. *J. Chem. Soc., Perkin Trans. 2* **1993**, 1557–1560.